Non parametric burning rate estimation

Henrik D. Nissen

Abstract:

Using a non parametric approach, it is possible to determine the burning rate / chamber pressure relationship for a particular composite propellant from measured pressure / time data obtained during testing in a variable burning area *characterization* motor. The numerical scheme for non parametric burning rate estimation avoids the problems of multidimensional minimization usually associated with parametric burning rate estimation and does not need an assumed burning rate / pressure relationship. These features ensure speedy and stable data analysis. The amount of information thus extracted from one test using a characterization motor with variabel burning area, is several times larger then possible with a constant area characterization motor, such as an endburner configuration.

Principle:

The nonparametric burning rate estimation algorithm is based on the following assumptions regarding the propellant, the combustion products and the grain geometry:

The burning rate $\partial s/\partial t$ is a singel valued function of the chamber pressure P_c, i.e. the propellant mixture does not vary and no erosive burning:

$$\dot{s} = f(P_c) \tag{A1}$$

Since the propellant mixture does not vary, neither does the propellant density ρ. The instantaneous combustion massflux $\partial m_b/\partial t$ from the propellant grain can then be expressed as:

$$\dot{m}_b \propto A_b \dot{s} \tag{A2}$$

Where A_b is the instantaneous burning area.

The combustion temperature and the combustion products are constant througout the burn. The combustion products consist of a mixture of ideal gases and incompressibel solids and liquids. This ensures that the specifik heats are constant while the combustion products travel through the nozzle. It can then be shown that the pressure and temperature at the throat will be a fixed ratio of their values in the cumbustion chamber. Since the internal energy in a mixture of ideal gases and incompressibel solids and liquids, only depend on the instantaneous temperature, the velocity in the throat of an ideal nozzle will be independent on the chamber pressure P_c. Since the throat temperature and combustion products mixture is constant, the density at the throat will be proportional to the chamber pressure P_c.

This gives the following relation for the exhaust massflux $\partial m_t/\partial t$ from the motor:

$$\dot{m}_t \propto A_t P_c \tag{A3}$$

Where A_t is the throat area.

Assuming quasi stationary combustion and nozzle flow, the combustion massflux must be equal to the exhaust massflux:

$$\dot{m}_t = \dot{m}_b \tag{A4}$$

The burning thoat area A_t is constant and the burning area A_b is a monotomically increasing function of the burning distance s from start at $s = 0$ to end at $s = s_{total}$:

$$A_t = constant \quad \wedge \quad A_b = A_b(s) \quad \wedge \quad \frac{\partial A_b}{\partial s} > 0 \quad , \quad 0 \le s \le s_{total} \tag{A5}$$

Using the above assumptions (A1) - (A5), the objective of the data analysis is to determine the burning rate function $f(P_c)$ given an experimentaly obtained chamber pressure / time curve $P_c(t)$, appriori known burning area $A_b(s)$ and total burning area s_{total} .

Combining (A2), (A3) and (4) gives:

$$A_t P_c = c_{ex} A_b \dot{s} \tag{1}$$

Where c_{ex} is a constant "exhaust" coefficient, dependning on the propellant and combustion product composition and combustion temperature.

Inserting (A1) gives:

$$A_t P_c = c_{ex} A_b f(P_c) \tag{2}$$

Given the start and end times for the combustion (t_0 and t_1) , which can be obtained from the measured pressure / time curve $P_c(t)$, a nonlinear ordinary differential equation for the burn distance with time varieing coefficients can then be obtained from (1):

$$\dot{s}(t) = \frac{A_t P_c(t)}{c_{ex} A_b(s(t))} \quad , \quad s(t = t_0) = 0 \tag{3}$$

Integrating this from t_0 to t_1 , gives the total *predicted* burning distance s_t :

$$s_t = \int_{t_0}^{t_1} \frac{A_t P_c(\tilde{t})}{c_{ex} A_b(s(\tilde{t}))} d\tilde{t} \tag{4}$$

Since the only parameter in this equation is the exhaust coefficient c_{ex} , this can be determined by equating the appriori known total burning distance s_{total} , with the *predicted* total burning distance given by s_t :

$$0 = s_{total} - s_t(c_{ex}) \tag{5}$$

Since this corresponds to solving a nonlinear equation with one variabel (c_{ex}), this is easily done numericaly.

After determining the exhaust coefficient c_{ex} , the burning rate $f(P_c)$ in the entire test pressure interval can then be determined by solving (3):

$$f(P_c(t)) = \dot{s}(t) = \frac{A_t P_c(t)}{c_{ex} A_b(s(t))} \quad , \quad s(t = t_0) = 0 \tag{6}$$

If the burning area A_b is monotomically increasing, the pressure will also increase monotomically unless the burning rate / pressure function is strongly decreasing (which is unlikely). Thus every pressure on the $P_c(t)$ curve will result in a burning rate $f(P_c)$, that will be a single valued function of the pressure, as assumed in (A1).

Case study:

As a practical example of this procedure, the pressure curve from a test of 30% Epoxy and 70% AP will be used. This test was conducted on 25 may 1998, and designated fm0398.

The pressure curve is shown below:

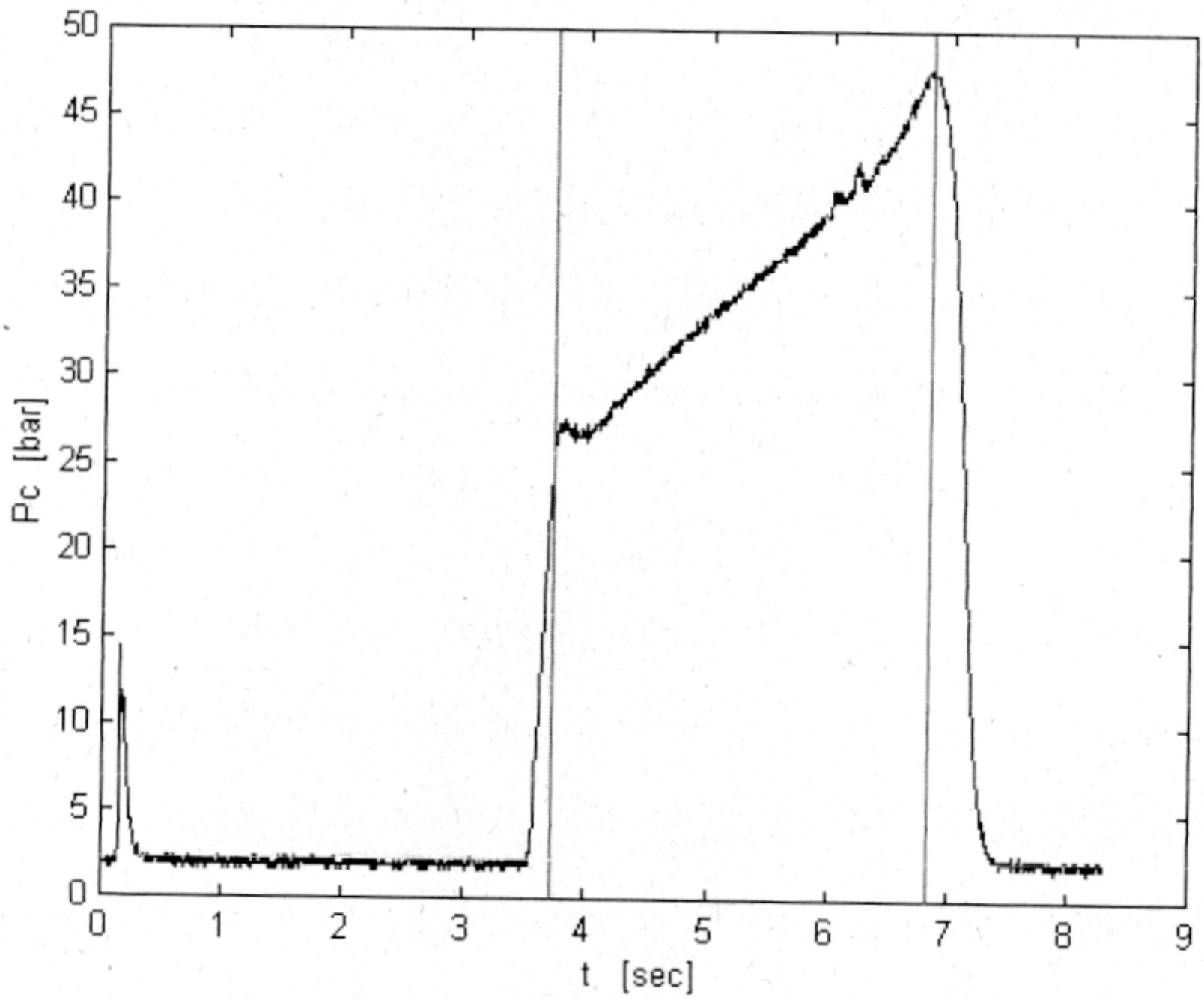

Fig. 1.

The chosen start and stop times t_0 and t_1 are marked on the pressure curve and given below:

$$\underline{t_0 = 3.72\,s} \quad \wedge \quad \underline{t_1 = 6.83\,s} \quad . \tag{C1}$$

The choice of start and stop times is somewhat intuitive, but in general the start time should be choosen to coincide with the start of propellant grain combustion (and not ignition) and the end time should correspond to the time where the combustion front first reaches the outer coating (for a hole burner). The choice of end time is driven by the need to know the current burning area, which may be erratic after the outer coating has been reached. Later it will be shown how to correct for the "afterburn" distance after the end time.

The nominel geometry for this particular grain is a circular cylindrical hole burner coated on the ends and the outside. The nominel burnarea is the inner perimeter of the hole. Since the perimeter of a cylindrical hole is proportional to the diameter, the burnarea function $A_b(s)$ varies linearly between the start area A_{b0} and the end area A_{b1} . The nominelle total burnlength is s_{total} . The following table summarizes the appriori known parameters of this particular test:

A_{b0}	A_{b1}	s_{total}	A_t
136.7 cm^2	245.9 cm^2	2.00 cm	0.709 cm^2

Using these data we may use the non parametric burning rate algorithm described above directly on the raw pressure file. Since $P_c(t)$ is known from the test and the burning rate $(\partial s/\partial t)(t) = f(P_c(t))$ is obtained from (6), a plot of $(\partial s/\partial t)(t)$ against $P_c(t)$ may be produced in the pressure interval obtained during the test:

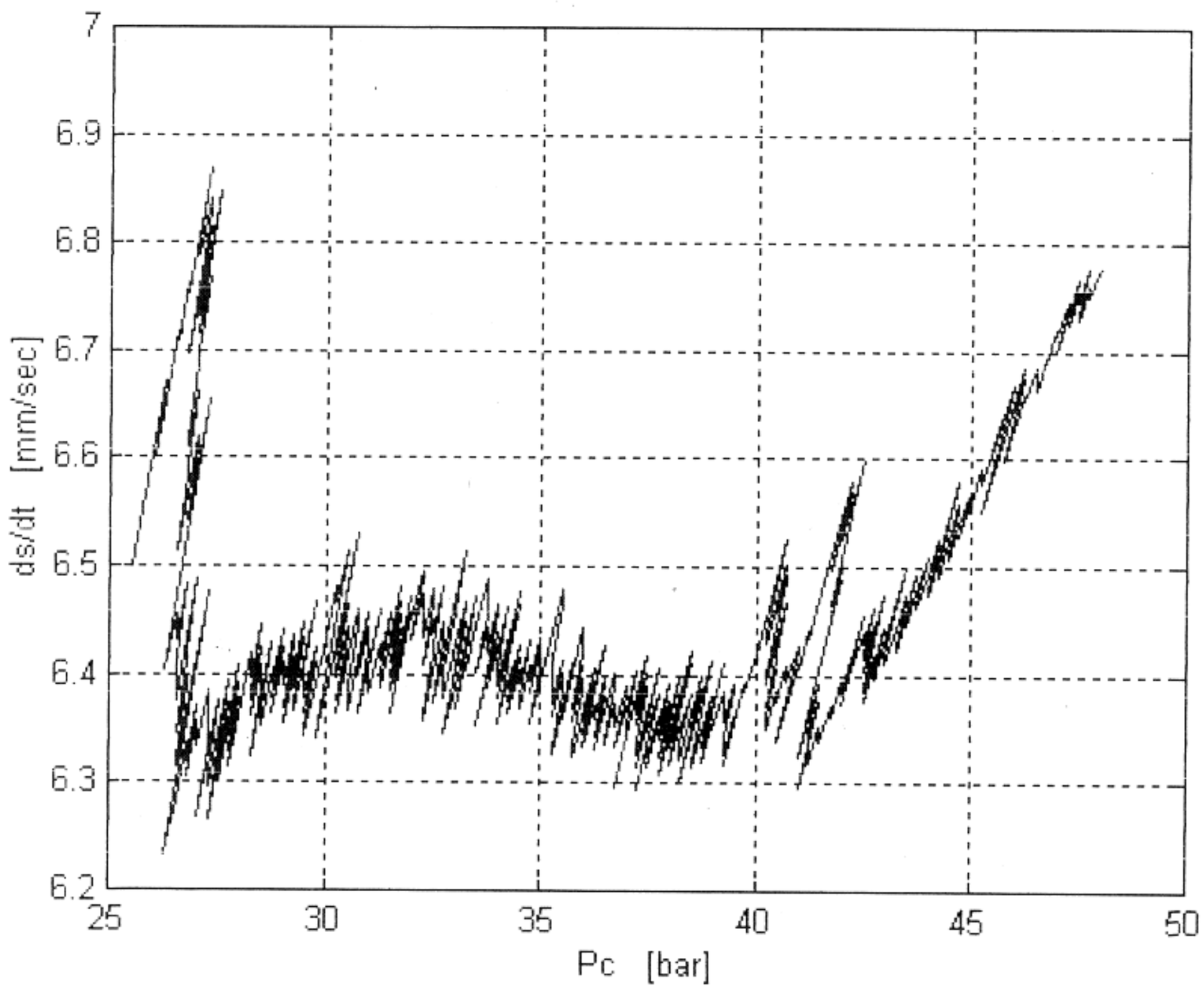

Fig. 2.

It is clear that there is a definite trend in the data but also a great deal of "noise". Two different problems are apparant; a high frequency apparantly random noise and an unphysical rapid fall in the burning rate at the lower end of the pressure interval, corresponding to the start of the burn. Comparing to the measured pressure curve in fig. 1. , it is apparant that the predicted rapid fall in burning rate is associated with the a start up phenomena (the "hump") seen in the measured pressure curve.

Preprocessing & filtering:

The problems encountered by the direct approache above may be solved by suitable preprocessing of the pressure file before using the non parametric burning rate algorithm:

Removal of unphysical samples:

The "hump" at the beginning of the pressure curve may be removed by using the requirement that the pressure must be monotomically increasing during the entire burn:

$$\frac{\partial P_c}{\partial t} > 0 \quad , \quad t_0 \le t \le t_1 \tag{7}$$

This condition can however not be used directly to remove any samples because of the high frequency noise in the measured pressure data. Instead the pressure file must first be filtered using a suitable low pass filter to remove the high frequency noise, taking care not to remove the underlying information.

One possibility is to fit a high order polynomial to the measured data and remove the data points from the measured data at places where the polynomial has a negative slop corresponding to a negative pressure/time slop. Using this procedure iteratively until the polynomial fit has a positive slop everywhere during the combustion time, gives a pressure file "cleaned" of unphysical samples.

Removal of high frequency noise:

The high frequency noise can be removed from the cleaned pressure file using a low order polynomial fit to the pressure data instead of the original data. The order of this fit is a compromise between removal of noise and preservation of burning rate data. Conversely it follows that the better the original data, the higher the order of the fit and the more burning rate data is obtained.

Case study (continued):

For the present case, the procedures above has been used to remove "unphysical" samples and high frequency noise. After some experimentation, a cleaning polynomial fit and a filtering fit of the following orders where found to produce a satisfactory filtered pressure/time file:

$$\underline{N_{clean} = 9} \quad \wedge \quad \underline{N_{filt} = 4} \tag{C2}$$

Where N_{clean} is the order of the "cleaning" and N_{filt} is the order of the final "filtering" fit.

The resulting filteret pressure can then be compared to the original measured data as seen in the following pressure/time graph:

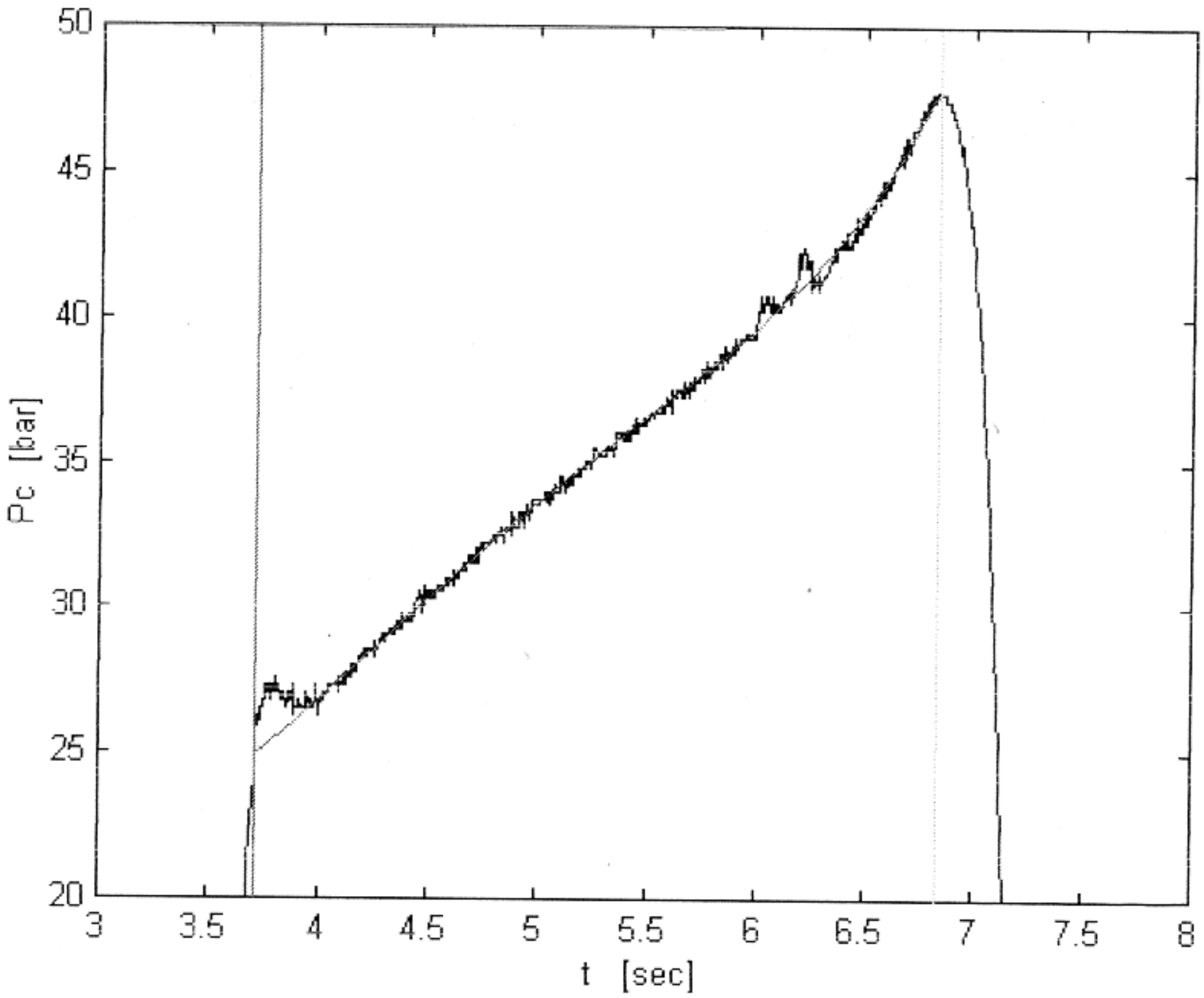

Fig. 3.

It can be seen that the fit is quit "good", in the sense that the effct of the initial "hump" has been minimized as well as the high frequency noise, while the major features of the original data has otherwise been preserved well. Since the filteret pressure curve is monotomically increasing, the resulting burnrate will be a single valued function of the chamber pressure.

Using the filteret measurements as a basis for the non parametric burn rate estimation, gives the following results:

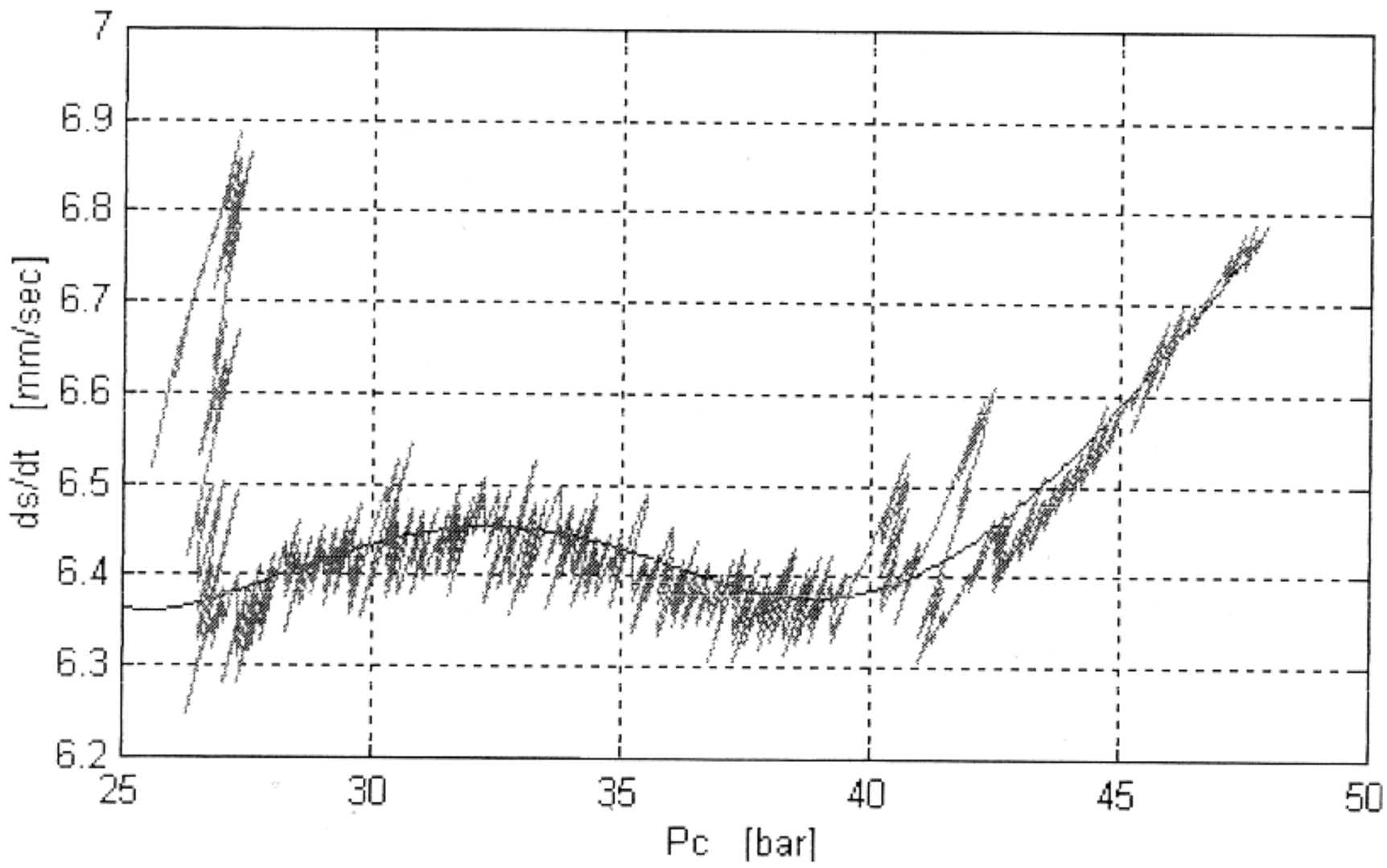

Fig. 4.

Where the original burnrate from the raw measurements are shown in the same plot for comparison.

Estimation of "afterburning" distance:

As indicated above, no knowledge of the burning area relationship $A_b(s)$ exists after the outer coating (in a hole burner) has been reached. However from the above analysis, the burning rate $(\partial s/\partial t) = f(P_c)$ is known at any chamber pressure encountered during the interval from t_0 to t_1 (as given in Fig.4). Thus the total total "afterburning" distance s_{after} may in principle be found by integrating the burning rate from t_1 to the end of measureble combustion (defined by ex. Pc = 5 bar):

$$s_{after} = \int_{t_1}^{t_2} f(P_c(\tilde{t}))\,d\tilde{t} \quad , \quad P_c(t_2) = 5\,bar \quad , \quad t_2 \geq t_1 \tag{8}$$

The afterburning distance can in the case of a hole burner be interpreted as a measure of the misalignment between the start hole and the outer coating. A simple example would be an excentricly located starting hole. In this case en excentricity of ϵ would result in an after burning distance of 2ϵ. Thus the *apparant* excentricity ϵ may be defined as:

$$\epsilon = \tfrac{1}{2} s_{after} \tag{9}$$

Since the burning rate $f(P_c)$ is not known when the pressure is below the smallest pressure encountered during the interval from t_0 to t_1 (designated P_0), the burning rate must be guessed. Alternatively

we may find the upper and lower bounds s_{a1} and s_{a2} on the afterburning distance, using zero and $f(P_0)$ respectively as the burning rates when $P_c < P_0$.

Case study (continued):

In the present case, the upper and lower bounds on the after burning distance become:

$$\underline{\underline{s_{a1} = 1.9\ mm}} \quad \wedge \quad \underline{\underline{s_{a2} = 2.9\ mm}} \tag{C3}$$

The apparant excentricity was thus of the order of 1-1.5 mm, which is within the tolerances for the propellant grain mold used.

Simple after burning correction:

If the afterburning distance is assumed to be some kind of geometrical misalingment, it follows that the burning surface might be assumed to be close to ideal until the burning surface reaches the outer coating. Since only the pressure measurements until this time has been considered when estimating the burning rate (remember choice of t_1), a first order correction of the total burning length can be expressed as:

$$s_{total\sim} = s_{total} - s_{after} \tag{10}$$

Where $s_{total\sim}$ is the after burning corrected total burndistance.

Since the ideal burning area varies linearly between A_{b0} and A_{b1} , and the burning surface is considered ideal until $s = s_{total\sim}$. The resulting end burning area corrected for afterburning becomes:

$$A_{b1\sim} = (A_{b1} - A_{b0}) \frac{s_{total\sim}}{s_{total}} + A_{b0} \tag{11}$$

Since the after burning distance is expressed as an upper and lower bound, this reults in two sets of modified burning geometries given by (10) and (11). If the after burning distance is not small compared to s_{total} , this correction may be used iteratively to obtain more refined esimates of $A_{b1\sim}$ and $s_{total\sim}$ and the estimated burning rate $f(P_c)$.

Using these new geometries but the original filteret pressure measurements, the non parametric burning rate estimation may be performed again, giving improved estimates of $f(P_c)$ for the tested propellant. The result is an upper and lower bound on $f(P_c)$.

Case study (continued):

Using the afterburning distances given by (C3), the following corrected burning rates are obtained:

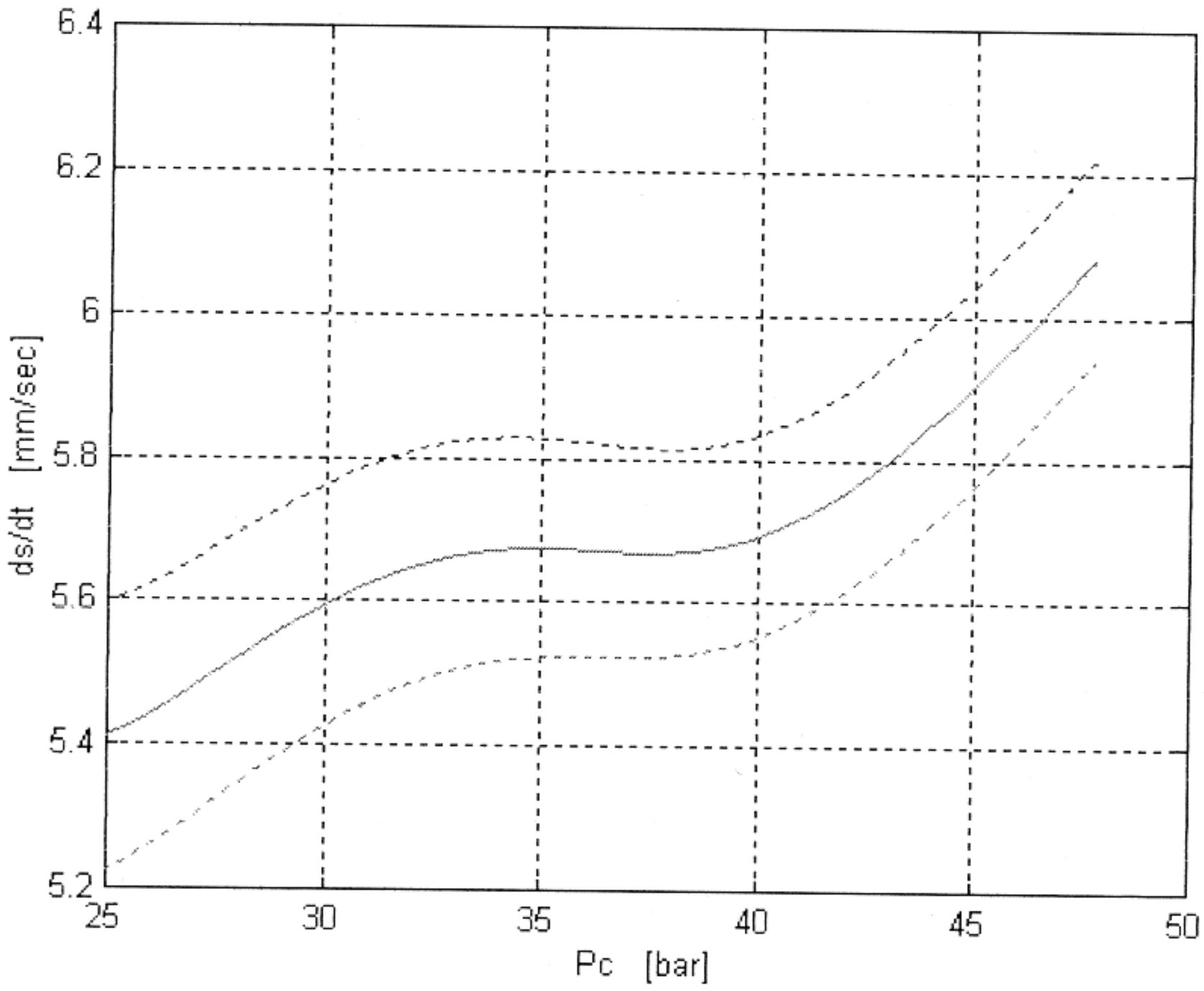

Fig. 5.

Where the dashed lines indicate the upper and lower bounds on the burning rate, and the solid line is the mean of the bounds.

Derived quantities:

With the burning rate determined in the entire chamber pressure range of the particular test, some usefull derived qauntities for the propellant may be determined in the same pressure range. Of particular usefullnes in the design of flight motors is the relationship between the ratio A_b/A_t and P_c. Using the value of the exhaust coefficient c_{ex} obtained in the proces of determining the burningrate, we may determine A_b/A_t as a function of P_c, by using (2):

$$\frac{A_b}{A_t} = \frac{P_c}{c_{ex}\, f(P_c)} \tag{12}$$

Another usefull quantity is the pressure exponent "n", which is an indicator of the pressure sensitivity of the burnrate for small pressure changes. The pressure exponent is defined in the following emperical burnrate/pressure model:

$$\dot{s} \approx cP_c^n \tag{12}$$

Where c and n are constants for the particular pressure range and propellant formulation.

Differentiation of (12) gives:

$$\frac{\partial \dot{s}}{\partial P_c} \approx cnP_c^{n-1} \tag{13}$$

Dividing (13) by (12) then gives:

$$n = \frac{\partial \dot{s}}{\partial P_c}\frac{P_c}{\dot{s}} \tag{14}$$

Substituting the estimated burningrate $f(P_c)$ into this gives the following expression for the pressure exponent:

$$n(P_c) = \left(\frac{\partial f(P_c)}{\partial P_c}\right)\frac{P_c}{f(P_c)} \tag{15}$$

Since the upper and lower boundaries of the burnrate is known, this leads to upper and lower boundaries for $n(P_c)$ and $P_c(A_b/A_t)$.

Case study (continued):

The relation between (A_b/A_t) and P_c for the tested propellant is shown below:

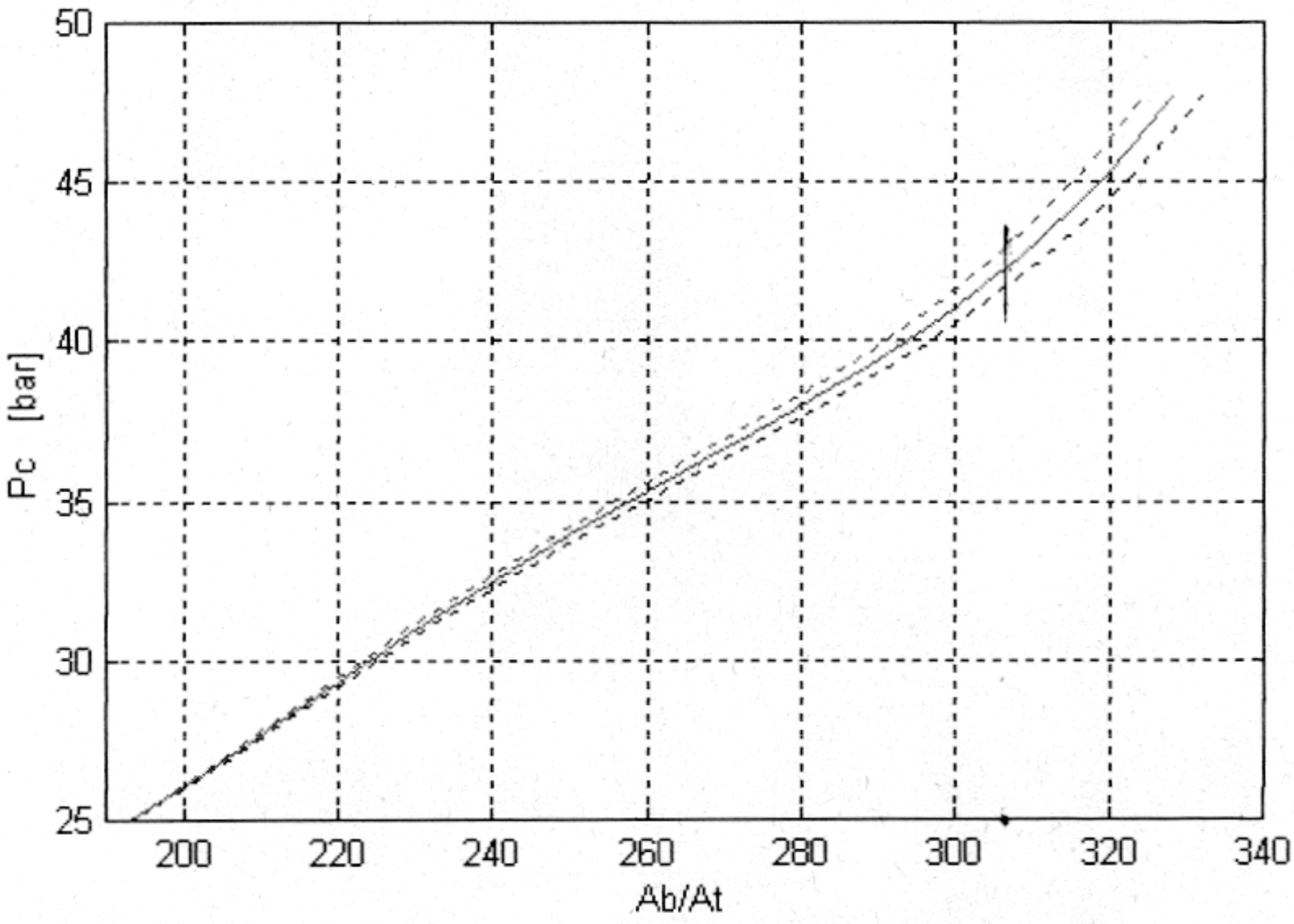

Fig. 6.

The uncertainty in the pressure is largest at the largest A_b/A_t values because these correspnd to the end of the burn, where the uncertainty in the burndistance is largest.

The pressure exponent $n(P_c)$:

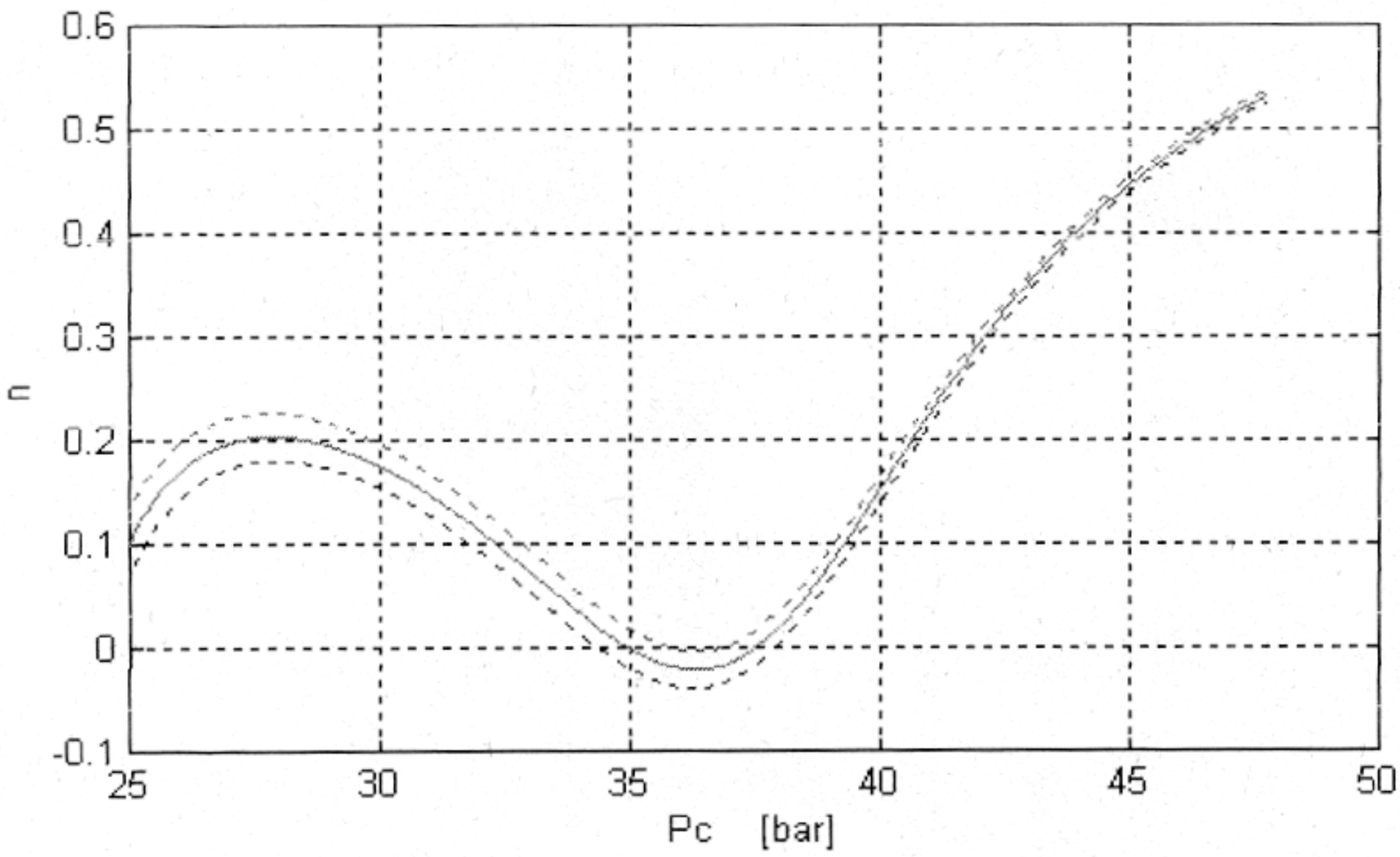

Fig. 7.

The plot of the pressure exponent should only be considered as a rough guideline, since the pressure exponent is determined using the differential of the burning rate $f(P_c)$. In the low and of the pressure interval, the actual pressure exponent may differ significantly from the values in fig. 7., because this pressure interval corresponds to the start of the burn. In this interval, the pressure is obtaned using extrapolation because of the "hump" in the original data (see fig. 3).

Instantaneous specific impulse:

If the thrust of the motor is obtained along with the pressure during testing, the specific impulse I_{sp} at each pressure obtained during the test may be determined if the propellant density ρ is known. The instantaneous massflux from the grain may be determined as:

$$\dot{m}_b(s) = \rho A_b \dot{s} = \rho A_b(s) f(P_c(s)) \tag{16}$$

Assuming quasi steady combustion and flow (A4):

$$\dot{m}_t(s) = \rho A_b(s) f(P_c(s)) \tag{17}$$

If the thrust is given as F(s) = F(t(s)), the instantaneous specific impulse is given as:

$$I_{sp}(s) = \frac{1}{g}\frac{F(s)}{\dot{m}_t(s)} \qquad [s] \tag{18}$$

Where g is the acceleration of gravity.

Since the chamber pressure is known at every burndistance from above, the specific impulse at any chamber pressure P_c in the test interval can be found using (18). The specific impulse does however

not *only* depend on the chamber pressure and the propellent, but also on the shape and size of the expansion part of the nozzle (specially the exit area to throat area relationship A_e/A_t).

Conclusion:

It has been shown how to determine the burning rate / chamber pressure relationship at any pressure encountered during a single test in a variable burning area characterisation motor. This is accomplished in a numerically stable way without assuming any burning rate / pressure model and without multidimensional minimization. It is also possible to correct for small unknown pertubations from the ideal grain geometry and obtain the $P_c(A_b/A_t)$ relationship at any A_b/A_t encountered during the burn. As extra information, a rough guide of the pressure exponent $n(P_c)$ may be obtained and providing thrust is also measured, the specific impulse $I_{sp}(P_c)$ may be determined.

not *only* depend on the chamber pressure and the propellent, but also on the shape and size of the expansion part of the nozzle (specially the exit area to throat area relationship A_e/A_t).

The characteristic velocity c^* is a constant for a given propellant mixture and only depends on the combustion products and the chamber temperature ['The potassiumnitrate-sugar prpellant', T.Vyverman,1978?]. The characteristic velocity is defined as:

$$c^* \equiv \frac{P_c A_t}{\dot{m}_t} \tag{19}$$

Rearranging this and comparing with (17) gives:

$$\dot{m}_t = \frac{P_c A_t}{c^*} = \rho A_b f(P_c) \quad \Leftrightarrow$$

$$P_c A_t = c^* \rho A_b f(P_c) \tag{20}$$

Comparing this with (2) gives a relationship between c^* and c_{ex} :

$$c_{ex} = c^* \rho \quad \Leftrightarrow \quad c^* = \frac{c_{ex}}{\rho} \tag{21}$$

Where c^* is expressed i m/s if c_{ex} and ρ are expressed in SI units.

Case study (continued):

In the present case the upper and lower boundaries on c_{ex} are determined as:

$$\underline{c_{ex1} = 0.0231\,bar{\cdot}s/mm = 2.31{\cdot}10^6 Pa{\cdot}s/m} \quad \wedge \quad \underline{c_{ex2} = 0.0248\,bar{\cdot}s/mm = 2.48{\cdot}10^6 Pa{\cdot}s/m}$$

(C4)

The density of the propellant has been determined as approximately $\rho = 1612$ kg/m^2 , (21) then gives the upper and lower boundaries on the characteristic velocity:

$$\underline{\underline{c_1^* = 1433\,m/s}} \quad \wedge \quad \underline{\underline{c_2^* = 1530\,m/s}} \tag{C5}$$

Conclusion:

It has been shown how to determine the burning rate / chamber pressure relationship at any pressure encountered during a single test in a variable burning area characterisation motor. This is accomplished in a numerically stable way without assuming any burning rate / pressure model and without multidimensional minimization. It is also possible to correct for small unknown pertubations from the ideal grain geometry and obtain the $P_c(A_b/A_t)$ relationship at any A_b/A_t encountered during the burn. As extra information, a rough guide of the pressure exponent $n(P_c)$ may be obtained and providing thrust is also measured, the specific impulse $I_{sp}(P_c)$ may be determined.